pISSN 1229-3008 eISSN 2287-6251
Progress in Superconductivity and Cryogenics
Vol.24, No.3, (2022), pp.24~29
https://doi.org/10.9714/psac.2022.24.3.024

A design study of a 4.7 T 85 mm low temperature superconductor magnet for a nuclear magnetic resonance spectrometer

Ryunjun Bae[a, b], Jung Tae Lee[*, a], Jeonghwan Park[a], Kibum Choi[a], and Seungyong Hahn[a]

[a] *Department of Electrical and Computer Engineering, Seoul National University, Seoul 08826, Korea*
[b] *Agency for Defense Development, Daejeon 34186, Korea*

(Received 19 November 2021; revised or reviewed 26 August 2022; accepted 27 August 2022)

Abstract

One of the recent proposals with nuclear magnetic resonance (NMR) is a multi-bore NMR which consists of array of magnets which could present possibilities to quickly cope with pandemic virus by multiple inspection of virus samples. Low temperature superconductor (LTS) can be a candidate for mass production of the magnet due to its low price in fabrication as well as operation by applying the helium zero boil-off technology. However, training feature of LTS magnet still hinders the low cost operation due to multiple boil-offs during premature quenches. Thus in this paper, LTS magnet with low mechanical stress is designed targeting the “training-free” LTS magnet for mass production of magnet array for multi-bore NMR. A thorough process of an LTS magnet design is conducted, including the analyses as the followings: electromagnetics, mechanical stress, cryogenics, stability, and protection. The magnet specification was set to 4.7 T in a winding bore of 85 mm, corresponding to the MR frequency of 200 MHz. The stress level is tolerable with respect to the wire yield strength and epoxy crack where mechanical disturbance is less than the minimum quench energy.

Keywords: low temperature superconductor magnet, magnet design, NbTi, nuclear magnetic resonance, training

1. INTRODUCTION

Nuclear magnetic resonance (NMR) is used in nuclear magnetic resonance spectroscopy, which is a useful method to determine the structure of molecules. NMR is widely used such as in drug discovery and development for pharmacy, protein structure analysis for biochemistry. For a better NMR spectroscopy performance, the main research and development (R&D) direction of NMR is to produce higher magnetic field to produce higher MR frequency which is actively being conducted by various institutes [1 – 7].

In a view of biomedical applications, a “Multi-bore NMR” concept has been proposed, which is array of NMR magnets in purpose to perform multiple NMR spectroscopies simultaneously [8]. This method is expected to deliver potentials to quickly cope with pandemic virus such as COVID-19 by multiple inspection of virus samples. The multi-bore NMR concept requires mass production of the superconducting magnet where LTS magnets are of potential candidates due to its merits over the HTS counterparts in its relatively lower fabrication cost. The operation cost of LTS magnet, usually recognized high owing to the increase of liquid helium cost, can also be lowered by adopting helium zero boil-off technology [9].

Before the normal operation, however, LTS magnet has to undergo various premature quenches, the so-called “training” [10]. It is in this operation stage where large liquid helium (LHe) consumption is inevitable even with helium zero boil-off technology. To avoid such dissipation of LHe, an LTS magnet with moderate size and field strength is designed to target a “training-free” NMR magnet which can make a mass production possible. It is well-known that 400 MHz NMR is the most widely utilized for spectroscopy due to its high price-spec ratio. But for multi-bore NMR application, we expect 200 MHz NMR has better potentials compared to 400 MHz NMR magnet [11] due to its: 1) > 6 times lower stored magnetic energy which corresponds to lower costs; 2) < 3 times volume resulting in higher compactness; 4) less complex configurations with less number of coils; 3) possible training-free features with lower mechanical stress.

200 MHz NMR magnet is designed in a thorough step-by-step manner to set as a starting point for multi-bore NMR development consisting four important aspects of superconducting magnets: 1) electromagnetics; 2) mechanical stress; 3) cryogenics; and 4) stability and protection. The magnet produces central magnetic field of 4.7 T which is the required for a 200 MHz NMR magnet with the selected Supercon’s NbTi MR24 wire. To improve the homogeneity of the magnetic field, harmonic analysis was performed, and two correction coils were applied. Stress analysis results showed that the magnet is mechanically stable withstanding the high Lorentz force. In cryogenics section, the amount of refrigerant used was calculated using both perfect mode and dunk mode. Lastly, enthalpy margin and minimum propagation zone (MPZ) were dealt with through stability analysis, and post quench analysis indicates that the magnet can be self-protected.

* Corresponding author: jtlee@snu.ac.kr

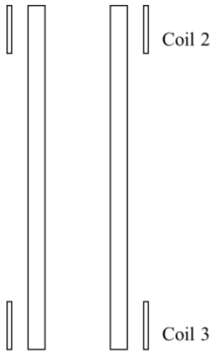

Fig. 1. The magnet consists of a main coil (Coil 1) and two correction coil (Coil 2 and Coil 3).

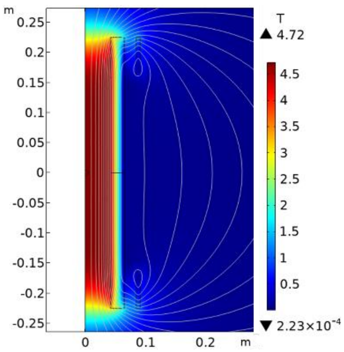

Fig. 2. Electromagnetic field density distribution of the magnet.

TABLE I
KEY PARAMETERS OF ELECTROMAGNETIC DESIGN

Conductor parameters	Units	Coil 1	Coil 2, Coil 3
Inner radius	[mm]	42.5	85
Outer radius	[mm]	65	91.5
Height	[mm]	450	63
Total turns		3375	124
Conductor usage	[km]	1.13	0.115
Total conductor usage	[km]	1.36	
Operation parameters			
Operating current	[A]	505	
Operating temperature	[K]	4.2	
Stored energy	[kJ]	33.3	
Engineering current density	[A/mm^2]	198	
Conductor current density	[A/mm^2]	217	
Filament current density	[A/mm^2]	1715	
Matrix current density	[A/mm^2]	249	

TABLE II
ELECTROMAGNETIC PERFORMANCE ESTIMATION

Performance parameters	Units	Value
Center field(@I_{op} = 505 A)	[T]	4.7
Minimum critical current	[A]	750
Magnet constant	[mT/A]	9.3
Field homogeneity(10 mm DSV)	[ppm]	0.14
Harmonic coefficients		
Z2	[T/mm^2]	3.464×10^{-8}
Z4	[T/mm^4]	4.069×10^{-11}
Z6	[T/mm^6]	-1.458×10^{-15}
Z8	[T/mm^8]	-1.636×10^{-19}
Z10	[T/mm^{10}]	-6.072×10^{-24}

2. ELECTROMAGNETICS

2.1. Electromagnetic(EM) Design

The 200 MHz LTS NMR magnet consists of three coils connected in series. Each coil is wound by the orthocyclic layer winding method and impregnated with epoxy. The coil shape is shown in Fig. 1. Coil 1 is the main coil that generates the magnetic field required for NMR, and Coil 2 and Coil 3 are correction coils added to improve field homogeneity. Table I shows the key parameters of the designed coil. The main coil was designed to have a radial thickness of 22.5 mm and a height of 450 mm. The inner radius of 42.5 mm was determined considering the room temperature bore diameter of 51 mm and additional radial space for cryostat, thermal shield, and bobbin. The total number of turns is 3375 for the main coil and 124 for each correction coil. The correction coil shape was designed for the purpose of attenuating secondary harmonics and is described in detail in the performance part. The designed magnet satisfies the central magnetic field requirement at an operating current of 505 A. The operating temperature is 4.2 K and the stored energy is 33.3 kJ. The current density was computed for each type: 1) engineering current density is 198 A/mm^2 and; 2) filament and matrix current densities are 1715 and 249 A/mm^2, respectively.

2.2. EM Performance Estimation

For electromagnetic analysis, Comsol, a commercial software based on finite element method, and in-house Matlab code were used. The central magnetic field for 200 MHz NMR corresponds to 4.7 T and the required field homogeneity is < 1 ppm. The field homogeneity without any correction coil was over 28 ppm, whereas after applying the correction coils to offset the second harmonics, the homogeneity performance was secured to ~ 0.14 ppm maintaining the magnitude of the central field to 4.7 T. Fig. 2 shows the magnetic flux density distribution.

Since it is a solenoid type magnet, B_z has the largest magnetic flux density at z = 0. From the calculated magnetic field distribution and the LTS wire's critical current data provided by the manufacturer, the minimum critical current of the magnet was found to be about 750 A at the inner most turn where the field is the maximum. Table II shows the parameters regarding electromagnetic performance.

2.3. Conductor Parameter

The superconducting wire for the 200 MHz NMR magnet was selected as NbTi MR 24 wire from Supercon. Table III shows the wire specification. The selected wire has a copper to NbTi ratio of 7:1 and consists of 24 filaments. The filament diameter is 125 μm, and the wire diameter is 1.72 mm in the bare state and 1.80 mm including insulation. The critical current at 5 T, 4.2 K was calculated by interpolating the manufacturer's data and is 700A. The magnetic field dependent critical current of the

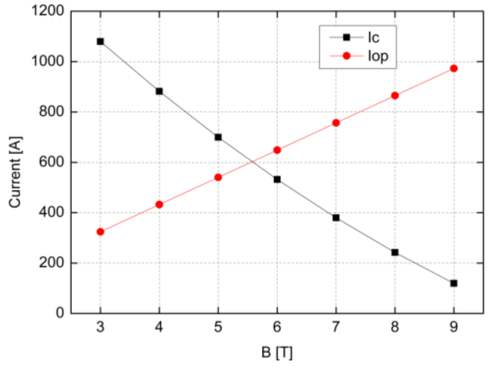

Fig. 3. The magnetic field dependent critical current of NbTi MR 24 wire at 4.2 K and the load line according to the operating current.

conductor at 4.2 K and the load line according to the operating current is shown in Fig. 3. The load line critical current is found to be 600 A.

TABLE III
CONDUCTOR SPECIFICATIONS

Parameters	Units	Value
Filament number		24
Cu:NbTi		7:1
Filament diameter	[μm]	125
Wire diameter	[mm]	1.72(Bare), 1.80(Insulated)
Critical current at 5 T, 4.2 K	[A]	700

TABLE IV
MECHANICAL PROPERTIES OF COMPOSITE CONDUCTOR

Mechanical parameters	Units	Value
E_h	[GPa]	42.5
E_r, E_z	[GPa]	41.7
Shear modulus	[GPa]	31.5
Poisson's ratio		0.33
Winding tension	[MPa]	3.85

3. SOLID MECHANICS

3.1. Mechanical Properties

In magnet stress analysis, the effect of the magnetic stress due to the Lorentz force and the winding tension were considered using the mechanical properties of composite conductor shown in Table IV.

The effective Young's modulus of the coil in hoop (E_h), radial (E_r), and axial (E_z) directions were calculated using the mixture rule for composite winding. The equations of mixture rule are represented as:

$$E_h = \frac{A_1E_1+A_2E_2}{A_1+A_2} \tag{1}$$

$$E_{r,z} = \frac{E_1E_2(L_1+L_2)}{L_1E_2+L_2E_1} \tag{2}$$

where A_1 and A_2 are the cross section area, E_1 and E_2 are Young's modulus, L_1 and L_2 are the length. The subscripts are, respectively, 1 for NbTi and 2 for copper. Shear modulus and Poisson's ratio were assumed to be 31.5 GPa and 0.33, respectively [12]. Also, the winding tension was assumed as 1kgf applied over the cross section of the wire's end.

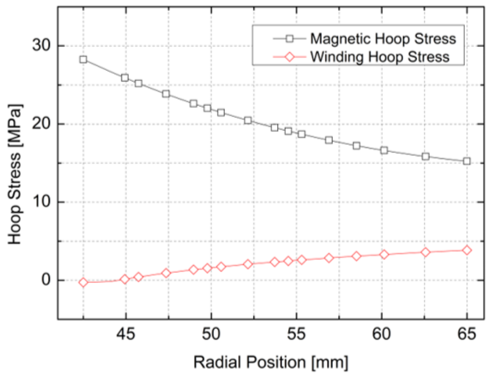

(a)

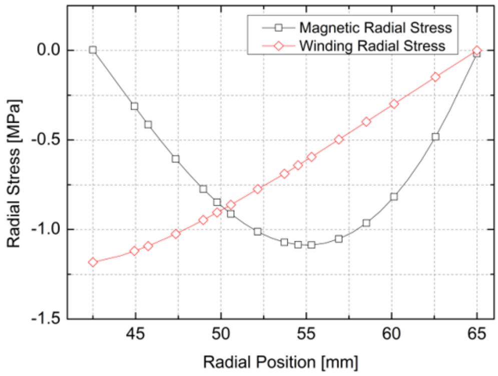

(b)

Fig. 4. Computed (a) hoop and (b) radial stresses of the designed magnet at z = 150 mm. The inner radius is 42.5 mm.

3.2. Stress-Strain Analysis

Stress analysis was performed using the finite element method, force equilibrium, and generalized Hooke's laws under the plane strain assumption. A roller condition was applied at z = 0 mm as a boundary condition. Fig. 4 and 5 show magnetic stress and strain, respectively. Magnetic hoop stress shows the peak value of 28.2 MPa at z = 150 mm in the innermost radius and tends to decrease as the radius increases. On the other hand, winding hoop stress tends to change from -0.2 MPa to 3.8 MPa as the winding progresses.

Since we are yet to decide specific epoxy material for winding, thermal stress is not considered for stress calculation. Additional thermal stress, which is expected to be compressive, may be tolerable considering the sum of electromagnetic and winding stress of 28 MPa and the yield strength of < 200 MPa for NbTi wire [13].

At the same position of peak hoop stress, the peak hoop strain is calculated to be 0.07% which is a value tolerable for critical current degradation; a degradation would hardly occur before ~ 0.2% of hoop strain [14]. For magnetic radial stress, which is tensile stress, the peak value reads 1.1 MPa. Winding radial stress, also tensile, has a peak

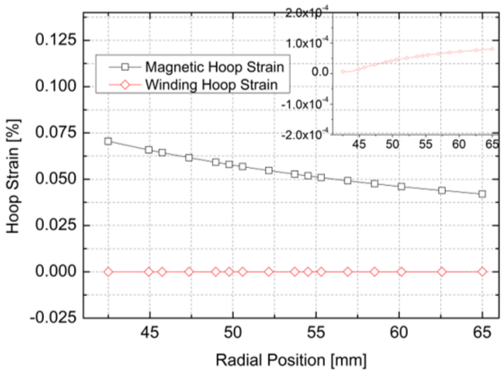

(a)

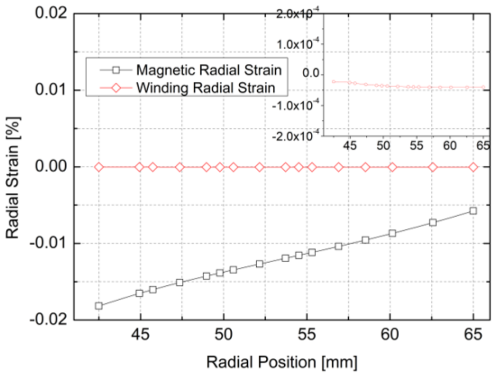

(b)

Fig. 5. Computed (a) hoop and (b) radial strains of the designed magnet at z = 150 mm. The inner radius is 42.5 mm.

value of 1.2 MPa in the innermost radius and gradually decreases and disappears at the point where the winding ends. This value can be considered tolerable regarding the tolerable radial tensile stress for epoxy is ~ 5 MPa [15].

Small magnets are known to have more advantageous characteristics than large magnets in training. In particular, solenoids of a few centimeters bore diameter typically have a current close to critical current at the first quench. Such training free characteristics can be expected from small solenoid magnets with bore of about 0.5 m or less [10]. The magnet designed in this research has a bore diameter of 85 mm for winding and is small enough to have training-free characteristics. In addition, according to the analysis results, the influence of mechanical disturbance with low peak stress is expected to be appropriate for maintaining this characteristic.

4. CRYOGENICS

In this section, the amount of cryogen to cool the magnet is estimated considering the enthalpy difference between the initial temperature (room temperature of 300 K) and the operation temperature (4.2 K). Here we have only considered the cooling of conductor winding since the structure is yet to be designed. Also, the heat input from the cryostat was neglected provided that sufficient shielding is done. They will be taken into account in further detailed design research.

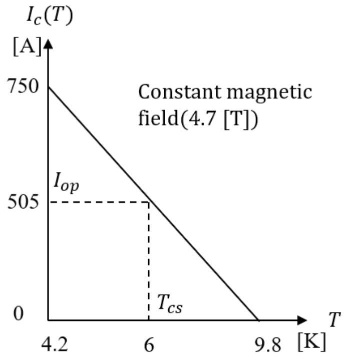

Fig. 6. Temperature versus critical current plot. Beyond 6 K, the current enters the region of current sharing through the matrix.

TABLE V
COOLING SPECIFICATIONS

	Units	Perfect mode	Dunk mode
LN2(300 ∼ 77 K)	[liter]	8.9	13.7
LHe(77 ∼ 4.2 K)	[liter]	4.5	62.5
Required cooling energy	[kJ]	2377	
Mass	[kg]	29.7 (NbTi: 2.4, Copper: 27.3)	

TABLE VI
STABILITY CHARACTERISTICS

	Units	Value
I_{co}	[A]	600
$i_{op} = I_{op}/I_{co}$		0.85
T_{cs}	[K]	6
Enthalpy margin	[J/cm^3]	4.2×10^{-3}
Minimum propagation zone	[mm]	13.9

The magnet is cooled with liquid helium (LHe). However, for an initial cool down the magnet is cooled by a two-step cool down procedure, using LN2 from 300 K to 77 K and LHe from 77 K to 4.2 K, to make the best use of the merit of liquid nitrogen (LN2) in both economic and thermodynamics perspectives. LN2 not only is an order of magnitude less expensive than LHe in volume but also has 60 times higher latent heat of vaporization. Under a "perfect" cool down mode, the magnet is cooled by a series of infinitesimal perfect energy exchange with refrigerant. An extreme mode of cool down is to "dunk" the whole magnet initially at T_i into a bath of refrigerant [15]. In perfect mode, 8.9 litter for LN2 and 4.7 litter for LHe is expected to be consumed, whereas in dunk mode, 13.7 litter for LN2 and 62.5 litter for LHe was calculated considering the required cooling energy of 2377 kJ. Cooling specifications are summarized in Table V.

5. STABILITY AND PROTECTION

5.1. Stability

Fig. 6 shows a critical current versus temperature plot. The operating current to load line critical current (I_{co}) ratio was calculated to be 0.85. The superconductor operates in a completely superconducting mode until the current sharing temperature (T_{cs}) is reached. Above T_{cs}, the current flowing through the superconductor also flows through the matrix composed of copper. The current flowing into the matrix generates joule heat, which causes a larger temperature rise [15]. To obtain T_{cs}, a linear approximation was used with the critical current being 0 A at 9.8K. The magnet designed in this paper has a temperature margin of 1.8 K, and current sharing starts from 6 K. Under adiabatic conditions, enthalpy margin was calculated to be 4.2 mJ/cm^3.

The minimum propagating zone (MZP) is the largest volume in which a magnet can maintain a superconducting state even if a normal state region occurs in the superconducting winding due to joule heating. The critical size of the hot spot that maintains the superconducting state can be estimated by the equation of MPZ, and the equation is represented as:

$$R_{m,z} = \sqrt{\frac{3k_{wd}(T_{cs}-T_{op})}{\rho_m J_m^2}} \tag{3}$$

where R_{mz} is the radius of a spherical MPZ. J_m, k_{wd} and ρ_m indicate matrix current density, thermal conductivity and resistivity of copper at 4 K, respectively. R_{mz} was calculated to be 13.9 mm and thus the minimum quench energy (MQE) was 47.2 mJ. If the hot spot size is smaller than R_{mz}, the generated heat is conducted along the wire axis and dissipated, and the normal state region returns to the superconducting state. Stability characteristics are summarized in Table VI.

A quantitative observation on training-free characteristic can be made through MQE and assumptions with mechanical disturbance by epoxy crack and wire motion within the hotspot volume ($V_{hotspot}$) and hotspot area ($S_{hotspot}$) [16]. First, the strain energy of the epoxy crack can be calculated as $1/2\,\sigma_r\epsilon_r V_{hotspot}$. Second, the energy dissipated during wire motion can be estimated with a friction energy density $\sigma_r\mu_k d S_{hotspot}$, where μ_k and d are kinetic friction coefficient and movement displacement, respectively. Assuming friction coefficient of 0.2 and displacement of 0.1 mm in transverse direction, the maximum mechanical disturbance energy within the winding is ~12 mJ which is about 1/4 of the MQE. This result may present possible training-free feature of the magnet upon nominal operation.

5.2. Protection

When the quench occurs in the superconducting magnet, the hot spot is generated, and the magnetic energy stored in the magnet is dissipated to the corresponding part and the temperature rises. At this time, the key to protection is to keep the rising temperature below the dangerous temperature, ~150 K. The final temperature T_f, which is raised by the adiabatic heating condition from the initial operating temperature T_i, can be obtained by the equation called the Z function [15]:

$$Z(T_f, T_i) = \int_{T_i}^{T_f} \frac{C_m}{\rho_m} dT \tag{4}$$

where C_m is the conductor's volumetric heat capacity.

Superconducting magnet protection methods can be broadly divided into passive and active. If the normal zone generated by quench rapidly diffuses throughout the magnet, that is, if the normal zone propagation (NZP) velocity is high, it is possible to prevent the magnetic energy stored in the magnet from being concentrated on the local hot spot. Consequently, if the maximum rise temperature is kept below 150 K, this can make the magnet self-protective. The NZP velocity can be obtained by the following equation.

$$U_l \approx \frac{J_m}{C_m(\tilde{T})}\sqrt{\frac{\rho_m(\tilde{T})k_m\tilde{T}}{(T_t-T_{op})}} \tag{5}$$

where $\tilde{T}$ is average temperature of the transition temperature, T_t = T_{cs}, and T_{op}, which is 5 K. The longitudinal NZP velocity of the designed magnet was calculated to be 45.4 m/s. Assuming that the transverse (turn-to-turn) NZP velocity U_t is $0.1U_l$, U_t is 4.54 m/s. Winding direction NZP time can be calculated by dividing the outermost winding tern length by Ul and its value is 4.5 ms. The NZP time in the radial direction can be calculated by dividing the distance between the outer radius and the inner radius by Ut, and its value is 4.95 ms. Applying the same method, the axial NZP time is 99.1 ms. Through this, it can be assumed that the normal zone generated in the magnet is completely diffused within 0.1 s.

The magnet must be protected in an appropriate way when the quench occurs. In current design, the superconducting magnet is separated from the power supply and the stability is confirmed under the adiabatic heating in magnet with shorted terminals in which internal magnetic energy is consumed by itself. The Z function in this condition can be expressed as follows.

$$Z(T_f, T_i) = \frac{1}{2}\left(\frac{A_m}{A_{cd}}\right)J_m^2\left(\frac{L}{R_{nz}}\right) \tag{6}$$

where A_m, A_{cd}, L, and R_{nz} are the cross-sectional areas of matrix and conductor, the inductance of the magnet with 0.26 H, and the constant normal zone resistance, respectively. R_{nz} is actually dependent on temperature, but for the sake of simplicity, it is regarded as a value at T_f and is represented as:

$$R_{nz} = f_r \frac{\rho_m(T_f)l_{total}}{4A_m} \tag{7}$$

where f_r is the fraction of the hot spot volume in the winding, and l_{total} denotes the total length of the coil.

To predict the final temperature T_f, f_r was assumed for two cases. First, since the NZP time is < 0.1 s, considering the case where the normal zone rapidly diffuses throughout the magnet and the entire volume has a resistance component, $f_r = 1$, T_f was calculated to be around 57 K.

Next, from a conservative point of view, f_r that causes the temperature of the magnet to rise to 149 K, at which the magnet is not permanently damaged, was calculated to be 0.054. When f_r reaches this value by the calculated NZP velocity, the magnet can be self-protecting, and the designed magnet satisfies the size limit of the self-protective magnet under the condition $f_r = 0.054$. The equation for size limit is as follows [15].

$$\frac{a_1(\alpha-1)}{U_t} < \frac{L}{R_{nz}} \tag{8}$$

where a_1 is the innermost winding radius, and α is aspect ratio of the outermost winding radius a_2 to a_1 (a_2/a_1).

6. CONCLUSION

This paper describes the design of a 4.7 T 85 mm bore low temperature superconductor magnet (LTS) for 200 MHz multi-bore nuclear magnetic resonance (NMR) spectrometer. The key design point was to generate center magnetic field of 4.7 T required for a 200 MHz NMR which can have low mechanical stress level to operate without premature quench due to mechanical disturbance.

For electromagnetic design, two correction coils were designed based on harmonic analysis to achieve homogeneity of 0.14 ppm. Considering the Lorentz force and the winding tension through stress analysis, the peak hoop strain and peak radial stress acting on the magnet under the operating current condition were tolerable. For the stability analysis of the magnet, the enthalpy margin was calculated showing a value of 4.2 mJ/cm^3 which corresponds to minimum quench energy of ~47.2 mJ. Based on the mechanical stress analysis, the mechanical disturbance was calculated to be ~12 mJ which conveys the possibility to operate the magnet without training. Post-quench analysis was also performed for the protection of the magnet. The results show that the peak temperature after quench under the adiabatic heating in magnet with shorted terminals was calculated to be 149 K for the conservative case where hotspot volume fraction is 0.054.

From the design results, the designed magnet is expected to operate stably with sufficient margin fulfilling the performance requirements. With the design basis of LTS magnet obtained through this study, we expect to have gained the potentials to develop LTS magnets for multi-bore NMR also contributing to the one of the starting point of this research direction.

ACKNOWLEDGMENT

This work was supported by National R&D Program through the National Research Foundation of Korea(NRF) funded by Ministry of Science and ICT(2022M3I9A1072846). This work was also supported in part by the Korea Medical Device Development Fund grant funded by the Korea government (the Ministry of Science and ICT, the Ministry of Trade, Industry and Energy, the Ministry of Health & Welfare, the Ministry of Food and Drug Safety) (1711138068, Project Number: KMDF_PR_20200901_0063).

REFERENCES

[1] J. Bascuñán, S. Hahn, Y. Kim, J. Song and Y. Iwasa, "90-mm/18.8-T All-HTS Insert Magnet for 1.3 GHz LTS/HTS NMR Application: Magnet Design and Double-Pancake Coil Fabrication," in *IEEE Transactions on Applied Superconductivity*, vol. 24, no. 3, pp. 1-4, June 2014, Art no. 4300904.

[2] M. Guan *et al.*, "A Parametric Study on Overband Radial Build for a REBCO 800-MHz Insert of a 1.3-GHz LTS/HTS NMR Magnet," in *IEEE Transactions on Applied Superconductivity*, vol. 26, no. 4, pp. 1-5, June 2016, Art no. 4301205.

[3] S. Hahn, J. Bascunan, W. Yao, and Y. Iwasa, “Two hts options for a 600 mhz insert of a 1.3 ghz lts/hts nmr magnet: Ybco and bscco,” *Physica C: Superconductivity and its applications*, vol. 470, no. 20, pp. 1721–1726, 2010.

[4] Piao, R., S. Iguchi, M. Hamada, S. Matsumoto, H. Suematsu, A. T. Saito, J. Li et al. "High resolution NMR measurements using a 400 MHz NMR with an (RE) Ba2Cu3O7− x high-temperature superconducting inner coil: Towards a compact super-high-field NMR." *Journal of Magnetic Resonance* 263 (2016): 164-171.

[5] Luchinat, Enrico, et al. "Protein in-cell NMR spectroscopy at 1.2 GHz." *Journal of biomolecular NMR, vol.* 75, no. 2, pp. 97-107, 2021.

[6] Y. Li, L. Wang and Q. Wang, "Electromagnetic Design of HTS Insert for Ultrahigh Field NMR Magnet," in *IEEE Transactions on Applied Superconductivity*, vol. 28, no. 3, pp. 1-5, April 2018, Art no. 4602105.

[7] K. L. Kim *et al.*, "400-MHz/60-mm All-REBCO Nuclear Magnetic Resonance Magnet: Magnet Design," in *IEEE Transactions on Applied Superconductivity*, vol. 26, no. 4, pp. 1-4, June 2016, Art no. 4302604.

[8] Jeonghwan Park et al., “Electromagnetic Analysis of HTS Magnet Array,” presented in 2022 Winter KIASC [O LA-II 1].

[9] Siemens Healthineers. Translate 7T Research Power Into Clinical Care with MAGNETOM Terra [Brochure], 2018.

[10] M. N. Wilson, *Superconducting Magnets.* New York: Oxford University Press Inc., 1983, p. 89.

[11] Y. Li *et al.*, "Analysis of Damage by Quench and Improvements in Rewinding for a 9.4-T Superconducting NMR Magnet," in *IEEE Transactions on Applied Superconductivity*, vol. 26, no. 1, pp. 1-5, Jan. 2016, Art no. 4300105.

[12] W. Gray and C. Sun, “Theoretical and experimental determination of mechanical properties of superconducting composite wire,” OAK RIDGENATIONAL LAB TN, Tech. Rep., 1976.

[13] Guan, Mingzhi, Xingzhe Wang, and Youhe Zhou. "Effects of cold-treatment and strain-rate on mechanical properties of NbTi/Cu superconducting composite wires." *SpringerPlus*, vol. 4, no. 1, pp. 1-7, 2015.

[14] J. Ekin, "Mechanisms for critical-current degradation in NbTi and Nb3Sn multifilamentary wires," in *IEEE Transactions on Magnetics*, vol. 13, no. 1, pp. 127-130, January 1977.

[15] Y. Iwasa, *Case studies in superconducting magnets: design and operational issues*. Springer science & business media, 2009.

[16] K. Seo and M. Morita, “Guidelines for LTS magnet design based on transient stability,” *Cryogenics*, vol. 45, no. 5, pp. 354-361, 2006.